Pergamon

0301-9322(95)00014-3

Int. J. Multiphase Flow Vol. 21, No. 5, pp. 861–873, 1995

0301-9322/95 $9.50 + 0.00

BUBBLE AND LIQUID FLOW CHARACTERISTICS IN A VERTICAL BUBBLING JET

M. IGUCHI[1], H. UEDA[2] and T. UEMURA[3]

[1]Faculty of Engineering, Osaka University, 2-1 Yamada-oka, Suita, Osaka 565, Japan

[2]Graduate School, Osaka University, 2-1 Yamada-oka, Suita, Osaka 565, Japan

[3]Faculty of Engineering, Kansai University, 3-3-35 Yamate, Suita, Osaka 564, Japan

(Received 23 February 1994; in revised form 13 February 1995)

Abstract—A vertical bubbling jet was formed in a cylindrical water bath by injecting air from a centric single-hole nozzle. Bubble characteristics, such as gas holdup (void fraction), bubble frequency, mean bubble rising velocity, mean chord length, were measured using a two-needle electro-resistivity probe. In addition, liquid flow characteristics, represented by the axial mean velocity, rms values of axial and radial turbulence components, Reynolds shear stress, effective kinematic viscosity, skewness and flatness factors for axial and radial turbulence components, were measured with a two-dimensional laser Doppler velocimeter.

The flow field in the bubbling jet was essentially classified into two regions with respect to the axial distance from the nozzle exit. One is located near the nozzle where the inertia force of injected gas plays an important role. The other is located far from the nozzle in which the buoyancy force of bubbles governs the flow. In this study the experimental results of liquid flow characteristics in the latter region were compared with those for a single-phase round jet. Turbulence production in the bubbling jet was found to mainly occur in the wake of bubbles and to be approximately two times as large as the turbulence production in the single-phase round jet. The turbulence structures for the two jets also were different from each other.

Key Words: two-phase flow, bubbling jet, electro-resistivity probe, LDV, gas holdup, relative velocity, Reynolds shear stress

1. INTRODUCTION

Gas injection into the bath of reactors has been widely used in a variety fields of engineering in order to promote mixing or chemical reactions. In particular, most current steelmaking processes are accompanied by gas injection (Mori & Sano 1981; Szekely *et al.* 1988; Iguchi *et al.* 1992). Two-phase flows in these processes are termed bubbling jet and are typical of gas–liquid two-phase flow with high temperature and high turbulence intensity. It is desired to measure the velocity of molten steel for the improvement of current processes as well as for the development of new processes. Measurement of the fluid flow velocity of molten metals is, however, very difficult at the present stage due to the lack of velocimetry applicable under these severe conditions. Accordingly various types of numerical simulations using turbulence models such as the k-ϵ model originally developed for single-phase flow have been performed to predict the flow field in steelmaking processes (Burty *et al.* 1990; Sawada *et al.* 1991). The validity of the numerical simulations has usually been examined by comparison with experimental results obtained using water as a model of steel, but none of them has received experimental confirmation in the two-phase flow region, i.e. in the bubbling jet region. This is because knowledge about turbulence characteristics containing Reynolds shear stress and higher order correlations is limited.

The effects of particles or bubbles on the turbulence structure in two-phase flows have been investigated extensively by many researchers; for example, Tsuji & Morikawa (1982), Tsuji *et al.* (1984), Gore & Crowe (1989), Kobayashi *et al.* (1991), Mizukami *et al.* (1992), Yuan & Michaelides (1992) and Yarin & Hetsroni (1994b) for solid–fluid two-phase flows in a duct, Serizawa *et al.* (1975a–c), Ohba & Yuhara (1982), Theofanous & Sullivan (1982), Marié & Lance (1983), Wang *et al.* (1987), Lee *et al.* (1989), de Bertodano *et al.* (1990, 1994), Kocamustafaogullari & Wang (1991), Lance & Bataille (1991), Kashinsky *et al.* (1993), Kataoka *et al.* (1993), Kataoka & Serizawa (1993) and Liu & Bankoff (1993) for gas–liquid two-phase flows in a duct and Modarress *et al.*

(1984), Parthasarathy & Faeth (1987), Mostafa (1992) and Yarin & Hetsroni (1994a,b) for solid-laden jets.

Compared with studies of the above-mentioned two-phase flows, bubbling jet studies are limited. Durst *et al.* (1986) mainly measured the mean rising velocities of gas and liquid for a bubble Reynolds number less than 100. Chesters *et al.* (1980), Iguchi *et al.* (1990a), Sheng & Irons (1991, 1992) and Gross & Kuhlman (1992) reported experimental results of the mean velocity components and the rms values of turbulence components. None of the previous investigators, however, has measured the Reynolds shear stress, skewness and flatness factors.

Meanwhile, Sun & Faeth (1986a,b) also investigated the mean velocity components and rms values of turbulence components of liquid in a bubbling jet. However, they generated the bubbling jet by premixing gas and liquid in a reservoir connected upstream of the nozzle, and hence the boundary condition at the nozzle is different from the present case.

In this study a vertical bubbling jet was generated in a cylindrical water bath by injecting air through a centric single-hole bottom nozzle. The gas flow rate was highly increased compared with the values in previous experiments by the present authors. The Reynolds shear stress, skewness factor and flatness factor were also measured using a two-dimensional laser Doppler velocimeter. The results were compared with published results for a single-phase free jet to reveal the effect of bubbles on the turbulence structure in a bubbling jet.

2. EXPERIMENTAL APPARATUS AND PROCEDURE

Figure 1 shows a schematic of the experimental apparatus. The acrylic cylindrical vessel had a diameter D of 20.0 cm and a height H of 40.0 cm. The inner diameter of the nozzle, d_{ni}, was 0.2 cm and the depth of water H_W was 25.0 cm. The injected air flow rate Q_G was adjusted by a mass flow controller at 41.4 or 296 N cm^3/s and thus a vertical bubbling jet was formed along the centerline of the bath. The origin of the co-ordinate system was placed at the center of the nozzle exit, and the axial and radial co-ordinates were denoted by z and r, respectively.

Gas holdup ϵ, bubble frequency f_B, mean bubble rising velocity $\bar{u}_B$ and mean chord length $\bar{L}_B$ were measured with a two-needle electro-resistivity probe system (Iguchi *et al.* 1990b). The output signal of the system was A/D converted and then processed on a 32 bit personal computer to determine $\epsilon, f_B, \bar{u}_B$ and $\bar{L}_B$.

The axial and radial velocity components were measured with a two-dimensional laser Doppler velocimeter (LDV) system. Details of the LDV system and the data processing method are reported elsewhere (Iguchi *et al.* 1994). The output signals of the LDV also were processed on a personal computer to obtain the axial and radial mean values, $\bar{u}$ and $\bar{v}$, the rms values of axial and radial turbulence components, u'_{rms} and v'_{rms}, Reynolds shear stress $\overline{u'v'}$, effective kinematic viscosity ν_{eff} and skewness and flatness factors of axial and radial turbulence components. The sampling number of data, N, was more than 3000 and the sampling time was longer than approximately 20 min at every measurement position.

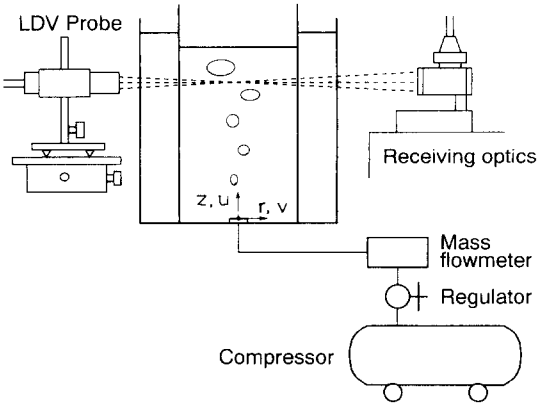

Figure 1. Experimental apparatus.

3. EMPIRICAL EQUATION OF REYNOLDS SHEAR STRESS IN VERTICAL BUBBLING JET

The present authors previously proposed a method of determining the effective kinematic viscosity ν_{eff} in a vertical bubbling jet from the governing equations based on the boundary layer approximation and the Boussinesq approximation (Iguchi & Morita 1991). The Boussinesq approximation assumes that bubbles affect the flow around themselves only through their buoyancy force. This approximation is considered to be valid in a low gas holdup region of the vertical bubbling jet.

The effective kinematic viscosity ν_{eff} based on the above-mentioned approximations is represented by

$$\nu_{eff} = 0.361 \left(g\epsilon_{cl} - \bar{u}_{cl}\frac{d\bar{u}_{cl}}{dz}\right)\left(\frac{b_u^2}{\bar{u}_{cl}}\right)\left\{1 - 0.5\left(\frac{r}{b_u}\right)^2\right\} \quad [1]$$

where g is the acceleration due to gravity, ϵ_{cl} is the centerline value of gas holdup ϵ, $\bar{u}_{cl}$ and b_u are the centerline value and the half-value radius of the axial mean velocity $\bar{u}$, respectively.

In deriving [1], $\bar{u}$ and ϵ were approximated by the following Gaussian error curves:

$$\bar{u} = \bar{u}_{cl}\exp\left(-\ln 2 \cdot \frac{r^2}{b_u^2}\right) \quad [2]$$

$$\epsilon = \epsilon_{cl}\exp\left(-\ln 2 \cdot \frac{r^2}{b_\epsilon^2}\right) \quad [3]$$

where b_ϵ is the half-value radius of gas holdup ϵ.

The Reynolds shear stress divided by fluid density can be given by

$$\overline{u'v'} \simeq -\nu_{eff}\frac{\partial \bar{u}}{\partial r} \quad [4]$$

4. EXPERIMENTAL RESULTS AND DISCUSSION

4.1. Bubble characteristics

Figure 2 shows the axial distributions of the centerline value ϵ_{cl} and the half-value radius b_ϵ of gas holdup for two gas flow rates. Measured values of ϵ_{cl} for each gas flow rate decreased abruptly near the nozzle and then decreased gradually as the axial distance from the nozzle exit increased. The inertia force of injected gas plays an important role near the nozzle exit, while the buoyance force of bubbles dominates in the axial region far from the nozzle exit (Iguchi *et al.* 1990a).

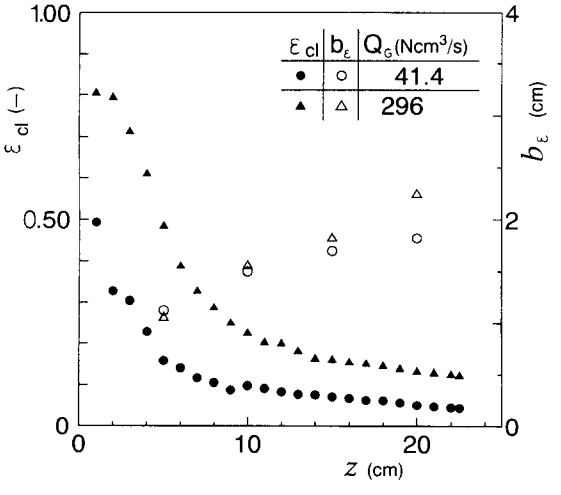

Figure 2. Axial distributions of the centerline value and half-value radius of gas holdup.

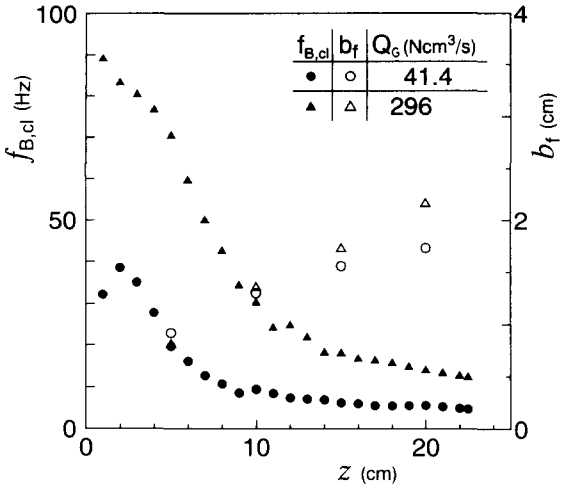

Figure 3. Axial distribution of the centerline value and half-value radius of bubble frequency.

Measured values of b_ϵ were hardly influenced by gas flow rate Q_G near the nozzle but the difference between b_ϵ values for the two gas flow rates increased with an increase in the axial distance z.

The centerline value $f_{B,cl}$ and half-value radius b_f of bubble frequency f_B are shown in figure 3. The change in $f_{B,cl}$ with respect to z was similar to that in ϵ_{cl}. The present authors have derived the following empirical equations for the frequency of bubble formation f_B and mean bubble diameter $\bar{d}_B$ at a nozzle or an orifice.

$$f_B = 1.06\left(\frac{\rho_L g^3}{\sigma}\right)^{1/4}\left(\frac{\rho_G}{\rho_L}\right)^{1/5}\left[\frac{(Q_G^2/g)^{1/5}}{d_{ni}}\right]^n \quad [5]$$

$$n = \begin{cases} 0.06\dfrac{z_{50}}{b_{\epsilon,50}} + 0.3 & \left(\dfrac{z_{50}}{b_{\epsilon,50}} \geqslant \dfrac{10}{3}\right) \\ 0.5 & \left(\dfrac{z_{50}}{b_{\epsilon,50}} < \dfrac{10}{3}\right) \end{cases} \quad [6]$$

$$z_{50} = a d_{ni} \mathrm{Fr}_m^b \quad [7]$$

$$b_{\epsilon,50} = c\left(\frac{Q_G^2}{g}\right)^{1/5} \quad [8]$$

$$\mathrm{Fr}_m = \frac{\rho_G Q_G^2}{\rho_L g d_{ni}^5} \quad [9]$$

$$a = 0.77\left(\frac{\rho_L}{\rho_G}\right)^{0.28} \quad [10]$$

$$b = 0.89\left(\frac{\rho_L}{\rho_G}\right)^{-0.16} \quad [11]$$

$$c = 0.26\left(\frac{\rho_L}{\rho_G}\right)^{0.07} \quad [12]$$

$$\bar{d}_B = \left(\frac{6Q_G}{\pi f_B}\right)^{1/3} \quad [13]$$

where ρ_L is the density of liquid, σ the surface tension of liquid, ρ_G the density of gas, z_{50} the axial distance at which $\epsilon_{cl} = 0.5$, $b_{\epsilon,50}$ the b_ϵ value at $z = z_{50}$ and Fr_m the modified Froude number.

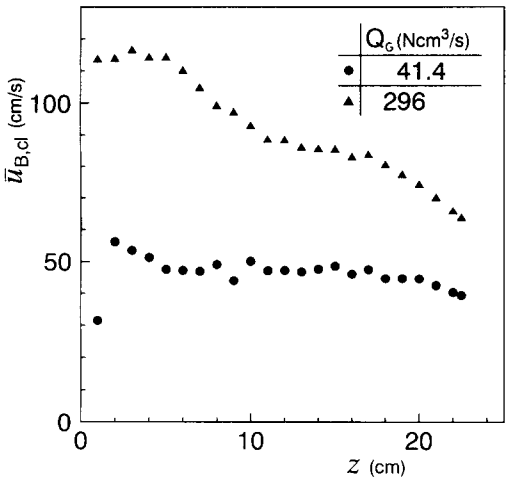

Figure 4. Distributions of mean bubble rising velocity on the centerline of the bath.

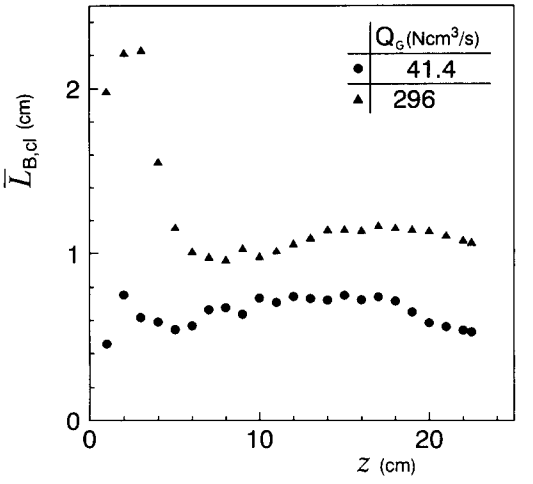

Figure 5. Distributions of mean chord length on the centerline of the bath.

Equation [5] gives $f_B = 41$ Hz for $Q_G = 41.4\,\mathrm{N\,cm^3/s}$ and 81 Hz for $Q_G = 296\,\mathrm{Ncm^3/s}$. The calculated value almost agreed with the measured value in the close vicinity of the nozzle for each Q_G. The measured value of b_f agreed well with that of b_c at every axial position.

Figure 4 illustrates measured values of bubble rising velocity on the centerline $\bar{u}_{B,cl}$. The measured values of $\bar{u}_{B,cl}$ for $Q_G = 41.1\,\mathrm{N\,cm^3/s}$ were almost uniform over the whole bath except in the bubble formation region near the nozzle, whereas two plateaus can be seen on the distribution for $Q_G = 296\,\mathrm{N\,cm^3/s}$.

The mean chord length on the centerline $\bar{L}_{B,cl}$ is shown in figure 5. Bubbles generated at the nozzle spread extensively in the radial direction near the nozzle and a part of each bubble disintegrated into smaller bubbles in the course of rising in the bath. As a result, $\bar{L}_{B,cl}$ decreased abruptly near the nozzle and then remained approximately constant in the buoyancy region. If every bubble is spherical in shape, the mean diameter of bubbles $\bar{d}_B$ becomes 1.5 times as large as $\bar{L}_{B,cl}$ (Kawakami *et al.* 1992).

In what follows, only the radial distributions of bubble characteristics at $z = 20$ cm, located in the buoyancy region, will be shown. The bubble characteristics near the nozzle will be discussed elsewhere.

As previously pointed out by many researchers (e.g. Kawakami *et al.* 1981; Castillejos & Brimacombe 1987), measured values of gas holdup and bubble frequency followed the Gaussian distribution as shown in figures 6 and 7. The abscissae in these figures were non-dimensionalized

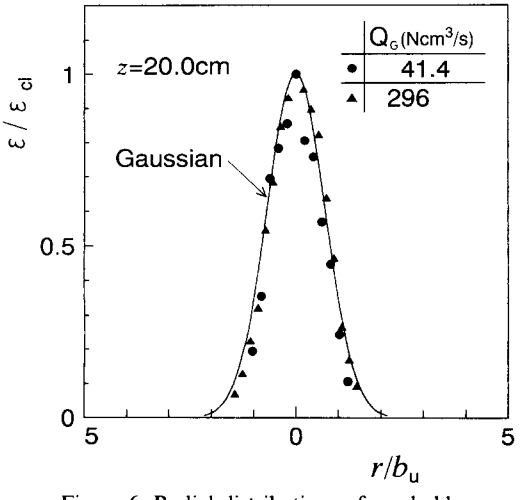

Figure 6. Radial distributions of gas holdup.

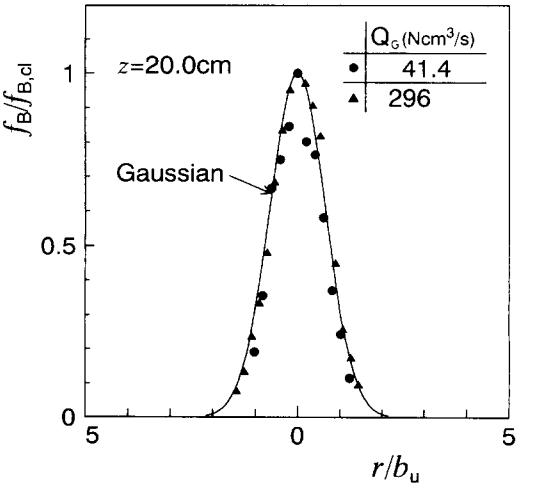

Figure 7. Radial distributions of bubble frequency.

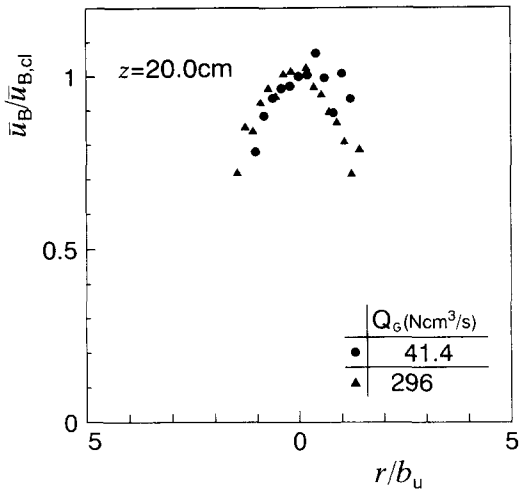

Figure 8. Radial distributions of mean bubble rising velocity.

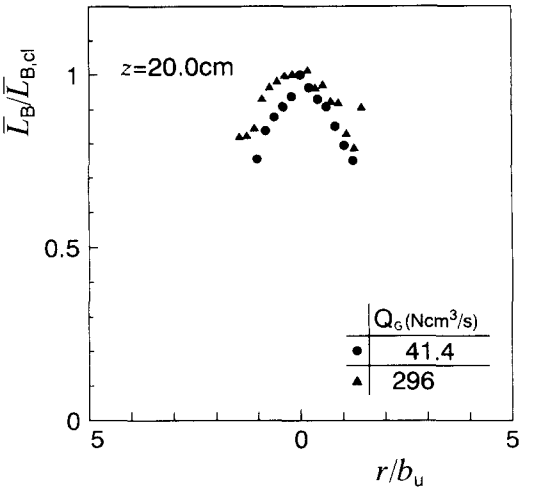

Figure 9. Radial distributions of mean chord length.

by the half-value radius b_u of the axial mean velocity $\bar{u}$. The data on b_u will be shown later. It is clear that bubbles exist in the radial region of $r/b_u \lesssim 1.5$.

Figures 8 and 9 plot the measured values of mean bubble rising velocity $\bar{u}_B$ and the mean chord length $\bar{L}_B$, respectively. Decreases in $\bar{u}_B$ and $\bar{L}_B$ in the radial direction were very small probably because bubbles ascended along zig-zag paths due to highly turbulent liquid motion.

4.2. Liquid flow characteristics

The axial distributions of $\bar{u}_{cl}$ and b_u are shown in figure 10. The measured values of $\bar{u}_{cl}$ for each gas flow rate changed in the axial direction in a similar manner to that for the mean bubble rising velocity on the centerline of the bath $\bar{u}_{B,cl}$. Although b_ϵ was an increasing function of Q_G, b_u was hardly affected by Q_G. That is, the radial extent of the region where water was moving upward was almost constant regardless of gas flow rate. Such an interesting phenomenon might be caused by the confinement effect of the side wall of the vessel.

In order to reveal the effect of the side wall on the liquid flow characteristics, water was injected into a water bath in the same vessel as shown in figure 1. This kind of jet is termed the single-phase confined jet. As will be shown later in figures 14 and 16, when b_u values for the two jets are almost equal, experimental results for the single-phase confined jet agree with those for the single-phase free jet in the radial region of $r/b_u \lesssim 1.5$. This fact implies that the liquid flow characteristics in

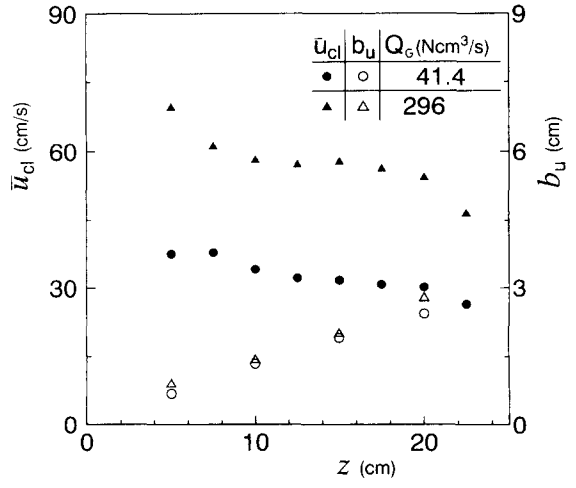

Figure 10. Distributions of axial mean velocity on the centerline of the bath.

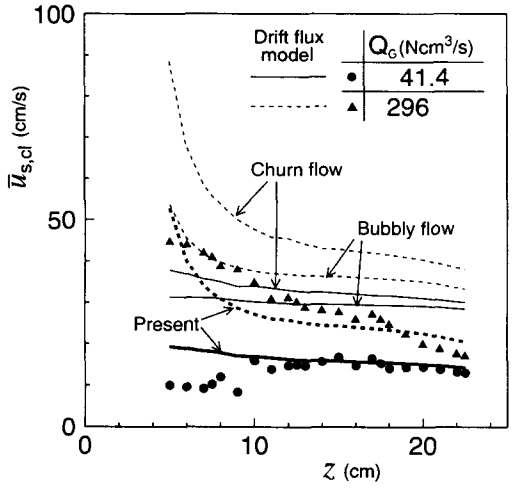

Figure 11. Distributions of relative velocity on the centerline of the bath.

this radial region are not influenced by the side wall. Therefore, it should be kept in mind that a comparison of the present experimental results for bubbling jet with those for the single-phase free jet is valid only in this radial region.

Figure 11 plots the so-called relative velocity on the centerline of the bath. The relative velocity $\bar{u}_s$ is defined as the difference between the mean bubble rising velocity $\bar{u}_B$ and the axial mean velocity of liquid $\bar{u}$. The dependence of $\bar{u}_{s,cl}$ on the gas flow rate was remarkable near the nozzle exit where the inertia force of injected gas governed the flow. The discrepancy for the two cases became small as z increased and $\bar{u}_{s,cl}$ approached about 20 cm/s for the two cases.

The so-called drift flux model has been widely used to predict the behavior of gas–liquid two-phase flow in a pipe. As far as the authors are aware, no drift flux model has been developed for bubbling jet. We therefore used the drift flux models for bubbly and churn flows in a pipe and examined their applicability to bubbling jet.

According to the drift flux model proposed for fully developed gas–liquid two-phase flow in a pipe (Ishii 1977), $\bar{u}_B$ is denoted by

$$\bar{u}_B = C_0[\epsilon\bar{u}_B + (1-\epsilon)\bar{u}] + V_{Gj} \quad [14]$$

$$C_0 = 1.2 - 0.2\left(\frac{\rho_G}{\rho_L}\right)^{1/2} \quad \text{(bubbly flow, churn flow)} \quad [15]$$

$$V_{Gj} = \begin{cases} (1-\epsilon)^{3/2}\sqrt{2}\left[\dfrac{\sigma g(\rho_L-\rho_G)}{\rho_L^2}\right]^{1/4} & \text{(bubbly flow)} \\ \sqrt{2}\left[\dfrac{\sigma g(\rho_L-\rho_G)}{\rho_L^2}\right]^{1/4} & \text{(churn flow)} \end{cases} \quad [16]$$

where C_0 is the distribution parameter and V_{Gj} is the drift velocity.

Under the present experimental conditions the distribution parameter C_0 and the drift velocity V_{Gj} reduce to

$$C_0 = 1.2 \quad \text{(bubbly flow, churn flow)} \quad [17]$$

$$V_{G_j} = \begin{cases} 23.1(1-\epsilon)^{3/2}\ \text{cm/s} & \text{(bubbly flow)} \\ 23.1\ \text{cm/s} & \text{(churn flow)} \end{cases} \quad [18]$$

The relative velocity $\bar{u}_{s,cl}$ can be expressed as follows:

$$\bar{u}_{s,cl} = \frac{0.2\bar{u}_{cl} + V_{Gj}}{1 - 1.2\epsilon_{cl}} \quad [19]$$

In figure 11 the drift flux model overestimates the relative velocity for each gas flow rate.

An attempt will be made to derive C_0 and V_{Gj} for bubbling jets. The distribution parameter C_0 seems to be insensitive to flow regimes. We therefore tried to adjust the drift velocity V_{Gj} to best fit the present measured values of the relative velocity. The results thus obtained are shown in figure 11, and C_0 and V_{Gj} are given by

$$C_0 = 1.2 - 0.2\left(\frac{\rho_G}{\rho_L}\right)^{1/2} \quad \text{(bubbling jet)} \qquad [15]$$

$$V_{Gj} = 0.5\left[\frac{\sigma g(\rho_L - \rho_G)}{\rho_L^2}\right]^{1/4} \quad \text{(bubbling jet)} \qquad [20]$$

Further discussion on the applicability of the drift flux model to bubbling jets should be left for a future study.

The rms values of the axial and radial turbulence components on the centerline of the bath, $u'_{rms,cl}$ and $v'_{rms,cl}$, are shown together in figure 12. For each gas flow rate $u'_{rms,cl}$ decreased slightly in the axial direction, whereas $v'_{rms,cl}$ remained almost constant in that direction. It is clear that $u'_{rms,cl} > v'_{rms,cl}$ everywhere in the bath just like the relation which holds for a single-phase round jet.

The turbulence intensity on the centerline of the bubbling jet was defined by

$$T_{u,cl} = \frac{u'_{rms,cl}}{\bar{u}_{cl}} \qquad [21]$$

Measured values of $T_{u,cl}$ were approximately 0.5 in the bubbling jet as shown in figure 13 just as mentioned in the previous paper (Iguchi *et al.* 1990a). It is known that $T_{u,cl}$ is about 0.25 in a single-phase round jet, and hence the turbulence intensity in the bubbling jet is almost twice the value in the single-phase jet.

Theofanous & Sullivan (1982) are first concerned with the relation between the turbulence intensity and relative velocity in bubbly flows in a vertical pipe and derived theoretically a correlation for it. More recently, Yuan & Michaelides (1992) and Yarin & Hetsroni (1994b) investigated theoretically the particles–turbulence interaction in dilute two-phase flows. However, no one has focused on the quantitative relation between the turbulence intensity and relative velocity in bubbling jet. Figure 13 also shows measured values of the ratio of the relative velocity to the axial mean velocity $\bar{u}_{s,cl}/\bar{u}_{cl}$. The measured values of $T_{u,cl}$ and $\bar{u}_{s,cl}/\bar{u}_{cl}$ are the same order of magnitude except near the nozzle for $Q_G = 41.4$ N cm^3/s. Therefore, we can conclude that the contribution of turbulence production in the wake of bubbles to the total turbulence production is dominant. That is, the contribution of the turbulence production due to entrainment of the surrounding liquid into the bubbling jet is weak.

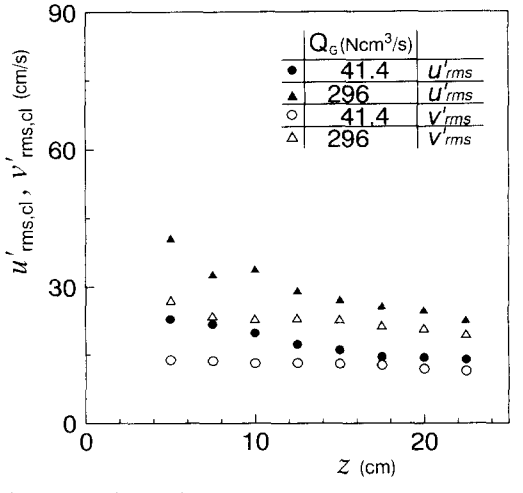

Figure 12. Distributions of root-mean-square values of the axial and radial turbulence components on the centerline of the bath.

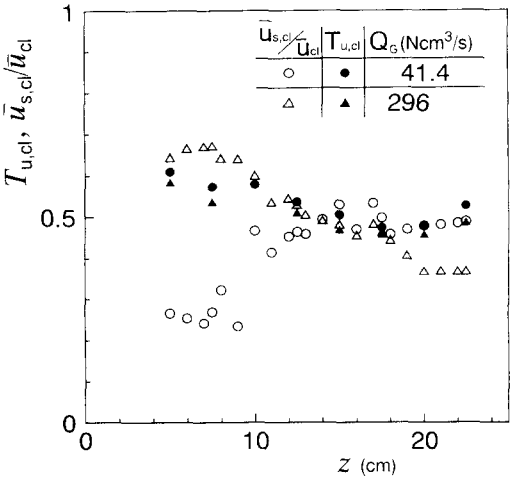

Figure 13. Comparison of turbulence intensity with the ratio of relative velocity to axial mean velocity on the centerline of the bath.

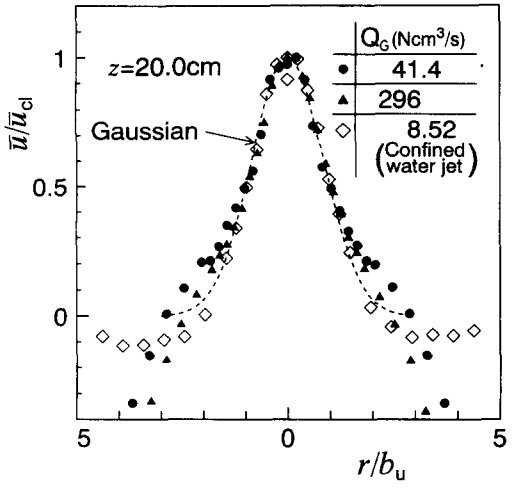

Figure 14. Radial distributions of axial mean velocity.

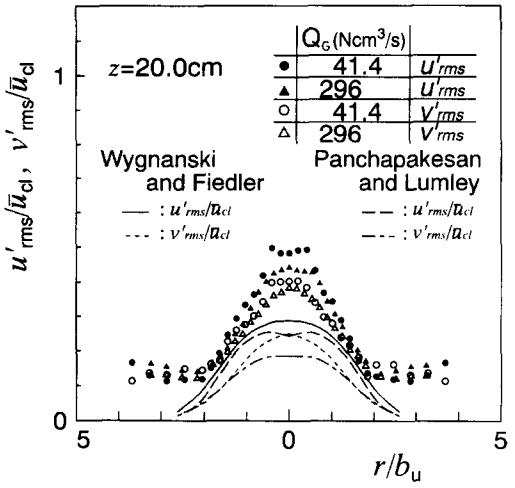

Figure 15. Radial distributions of root-mean-square values of the axial and radial turbulence components.

The radial distributions of the axial mean velocity $\bar{u}$ at $z = 20$ cm are shown in figure 14. The distributions for the two gas flow rates were similar and followed the Gaussian distribution, being valid for single-phase free jet, in the central part of the bubbling jet ($r/b_u \lesssim 1.5$). The measured values of single-phase confined jet also agreed with the free jet curve for $r/b_u \lesssim 1.5$.

Figure 15 illustrates the radial distributions of u'_{rms} and v'_{rms} at $z = 20$ cm. The four lines denote experimental results for single-phase jets (Wygnanski & Fiedler 1969; Panchapakesan & Lumley 1993). The rms values for the vertical bubbling jet are much larger than those for the single-phase jet. The measured rms values for the vertical bubbling jet never diminish at around the outer edge unlike those for the single-phase free jet. Such non-zero rms values were caused by the recirculating flow existing outside the bubbling jet.

Figure 16 shows the radial distributions of Reynolds shear stress. The Reynolds shear stress in the vertical bubbling jet was about two times as large as that in the single-phase jet. Since the turbulence production can be approximated by $\overline{u'v'}(\partial\bar{u}/\partial r)$, its value in the bubbling jet also is about twice as large as the single-phase jet value. The empirical equation based on the Boussinesq and the boundary layer approximations also underestimated the measured values for the bubbling jet.

The effective kinematic viscosity ν_{eff} was non-dimensionalized and is shown in figure 17. As expected, ν_{eff} in a bubbling jet was much larger than that in a single-phase round jet.

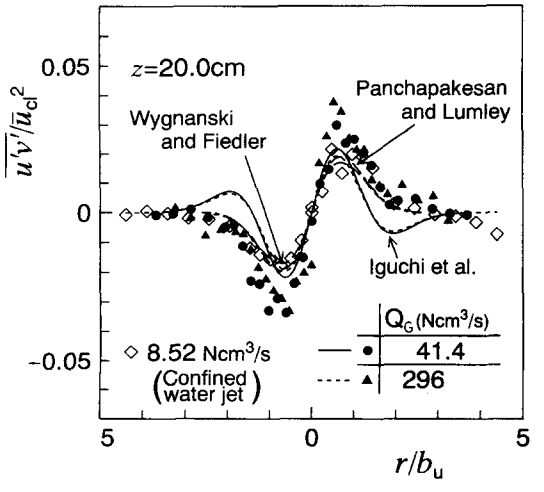

Figure 16. Radial distributions of Reynolds shear stress.

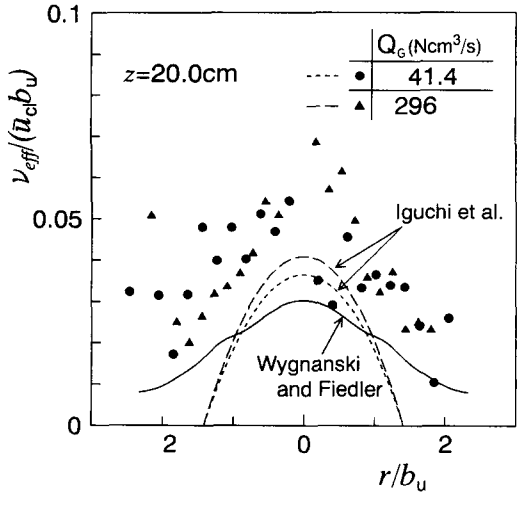

Figure 17. Radial distributions of effective kinematic viscosity.

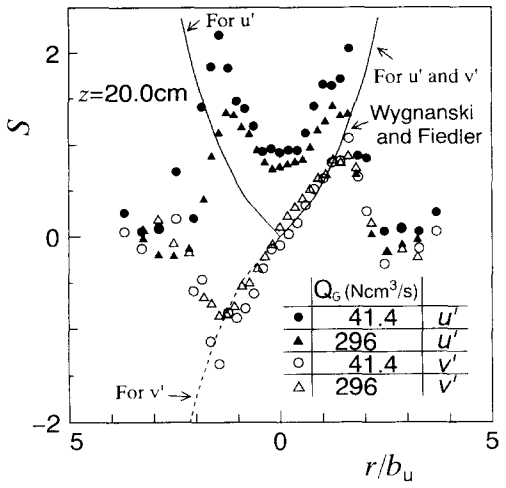

Figure 18. Radial distributions of skewness factor of the axial and radial turbulence components.

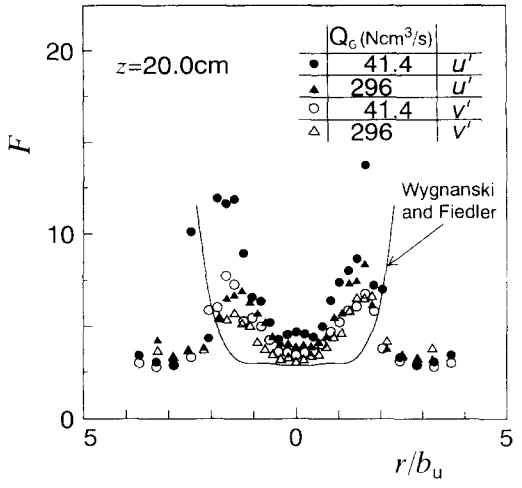

Figure 19. Radial distributions of flatness factor of the axial and radial turbulence components.

Figure 18 shows the skewness factor for the axial and radial turbulence components. Wygnanski & Fiedler (1969) found that the skewness factors for the two components were in good agreement with each other for a single-phase jet. The skewness factors can also be calculated from the recent work of Panchapakesan & Lumley (1993). The result shows that the skewness factor for u' is slightly larger than that for v' in the central part of the jet, though the result is not shown in figure 18 in order to avoid crowding in the figure. Concerning the skewness factors for a bubbling jet, in the radial region of $r/b_u \lesssim 1.5$, where rising bubbles existed and $\tilde{u}$ followed the Gaussian distribution just like the single-phase free jet, the skewness factor for v' almost agreed with the value for a single-phase jet, whereas the skewness factor for u' was different from that for v' and had a positive value of about 0.8. Such a difference appears to be caused by the turbulence production in the wake of bubbles. Outside the bubbling jet ($r/b_u \gtrsim 2.5$), both skewness factors for a bubbling jet became almost zero.

Figure 19 shows the radial distributions of flatness factor. The measured values of flatness factor for v' near the centerline of the bubbling jet were approximately three. As mentioned above, the skewness factor for v' was almost zero near the centerline. These facts mean that the probability distribution function for v' follows the Gaussian distributions ($S = 0$, $F = 3$) near the centerline of the bubbling jet. In the radial region of $r/b_u \gtrsim 2.5$, the flatness factor for u' was slightly larger than that for v'.

5. CONCLUSIONS

Measurements of bubble and liquid flow characteristics in an air–water vertical bubbling jet were made using a two-needle electro-resistivity probe and a two-dimensional LDV system for two gas flow rates of 41.4 and 296 N cm³/s. The main findings obtained in this study are summarized as follows:

(1) Gas holdup decreased abruptly near the nozzle and then decreased gradually in the axial direction. In the region near the nozzle the inertia force of injected gas plays an important role, while the buoyancy force of bubbles governs the flow in the region far from the nozzle. The limit between the two regions is represented by $z \simeq 5$ cm for $Q_G = 41.4$ N cm³/s and $z \simeq 10$ cm for $Q_G = 296$ N cm³/s. The axial distributions of bubble frequency, mean bubble rising velocity and mean chord length on the centerline of the bubbling jet also support this conclusion.

(2) The radial distributions of bubble characteristics were shown only for the buoyancy force dominant region located far from the nozzle. The radial distributions of gas holdup and bubble frequency were similar and followed the Gaussian distribution. The measured values of mean bubble rising velocity and mean chord length decreased slightly in the

radial direction. This is because bubbles rise along zig-zag paths due to highly turbulent liquid motion.

(3) The axial mean velocity $\bar{u}$ decreased gradually in the axial direction for the two gas flow rates. The distributions of relative velocity on the centerline, however, were different from each other. The difference was significant near the nozzle, but became small as z increased. On the other hand, the turbulence intensity on the centerline was approximately uniform ($\simeq 0.5$) in the bath. This value is much larger than the single-phase jet value of about 0.25. The ratio of relative velocity $\bar{u}_{s,cl}$ to axial mean velocity $\bar{u}_{cl}$ was almost the same as $T_{u,cl}$ except near the nozzle for $Q_G = 41.4$ N cm^3/s. This fact suggests that turbulence production mainly occurs in the wake of bubbles.

(4) The radial distributions of the axial mean velocity $\bar{u}$ for $Q_G = 41.4$ and 296 N cm^3/s were also similar and followed the Gaussian distribution in the central part of the bubbling jet. Measured values of the rms values of axial and radial turbulence components, u'_{rms} and v'_{rms}, Reynolds shear stress $\overline{u'v'}$ and effective kinematic viscosity ν_{eff} were approximately twice as large as those for single-phase free jets. Turbulence production was therefore much larger in a vertical bubbling jet than in a single-phase round jet.

(5) The skewness and flatness factors for the radial turbulence component v' in the central part of the bubbling jet were in good agreement with those for a single-phase jet ($S \simeq 0, F \simeq 3$). The probability distribution function of v' would therefore follow the Gaussian distribution. On the other hand, the skewness factor for u' was positive in the central part of the bubbling jet and the flatness factor for u' was larger than that of a single-phase round jet.

REFERENCES

de Bertodano, M. L., Lahey Jr, R. T. & Jones, O. C. 1994 Development of a k–ϵ model for bubbly two-phase flow. *Trans. ASME J. Fluids Engng* **116,** 128–134.

de Bertodano, M. L., Lee, S-J., Lahey Jr, R. T. & Drew, D. A. 1990 The prediction of two-phase turbulence and phase distribution phenomena using a Reynolds stress model. *Trans. ASME J. Fluids Engng* **112,** 107–113.

Burty, M., Fautrelle, Y. & Huin, D. 1990 A computational model for the prediction of turbulent recirculating two-phase flows. *Proc. 6th IISC Nagoya* **1,** 444–451.

Castillejos A. H. & Brimacombe, J. K. 1987 Measurement of physical characteristics of bubbles in gas–liquid plumes: part 2. *Metall. Trans.* **18B,** 659–671.

Chesters, A. K. Doorn, M. & Goosens, L. H. J. 1980 A general model for unconfined bubble plumes from extended sources. *Int. J. Multiphase Flow* **6,** 499–521.

Durst, F., Schönung, B., Selanger, K. & Winter, M. 1986 Bubble-driven liquid flows. *J. Fluid Mech.* **170,** 53–82.

Gore, R. A. & Crowe, C. T. 1989 Effect of particle size on modulating turbulent intensity. *Int. J. Multiphase Flow* **15,** 279–285.

Gross, R. W. & Kuhlman, J. M. 1992 Three-component velocity measurements in a turbulent recirculating bubble-driven liquid flow. *Int. J. Multiphase Flow* **18,** 413–421.

Iguchi, M. & Morita, A. 1991 Effective kinematic viscosity and effective diffusivity of bubbles in air–water bubbling jet. *Tetsu-to-Hagané* **78,** 66; *ISIJ Int.* **32,** 857–864.

Iguchi, M., Takeuchi, H. & Morita, Z. 1990a The flow field in air–water vertical bubbling jets in a cylindrical vessel. *Tetsu-to-Hagané* **76,** 699; *ISIJ Int.* 1991 **31,** 246–253.

Iguchi, M., Kawabata, H., Iwasaki, T., Nozama, K. & Morita, Z. 1990b Bubble characteristics in the momentum region of air–water vertical bubbling jet. *Tetsu-to-Hagané* **76,** 840; *ISIJ Int.* 1991 **31,** 952–959.

Iguchi, M., Nozawa, K., Tomida, H. & Morita, Z. 1991 Bubble characteristics in the buoyancy region of a vertical bubbling jet. *Tetsu-to-Hagané* **77,** 1426; *ISIJ Int.* **31,** 747–753.

Iguchi, M., Uemura, T. & Kondoh, T. 1994 Simultaneous measurement of liquid and bubble velocities in a cylindrical bath subject to centric bottom gas injection. *Int. J. Multiphase Flow* **20,** 753–762.

Iguchi, M., Uemura, T., Yamamoto, F. & Morita, Z. 1992 Multiphase flows in ironmaking and steelmaking processes. *Jpn. J. Multiphase Flow* **6,** 54–64.

Ishii, M. 1977 One-dimensional drift-flux model and constitutive equations for relative motion between phases in various two-phase flow regimes. *ANL* **77,** 47.

Kashinski, O. N., Timkin, L. S. & Cartellier, A. 1993 Experimental study of "laminar" bubbly flows in a vertical pipe. *Exp. Fluids* **14,** 308–314.

Kataoka, I. & Serizawa, A. 1993 Analyses of the radial distributions of average velocity and turbulent velocity of the liquid phase in bubbly two-phase flow. *JSME Int. J.* **36B,** 404–411.

Kataoka, I., Besnard, D. C. & Serizawa, A. 1993 Analysis of turbulence spectra in gas–liquid two-phase flow. *30th Jpn. Nat. Symp. Heat Transfer*, p. 94–96.

Kawakami, M., Tomimoto, N. & Ito, K. 1982 Statistical analysis of gas bubbles dispersion in liquid phase—water model experiment on bottom blowing processes. *Tetsu-to-Hagané* **68,** 774–783.

Kawakami, M., Hosono, S., Takahashi, K. & Ito, K. 1992 Bubble dispersion phenomena in water, mercury, molten iron and molten copper baths. *Tetsu-to-Hagané* **78,** 267–274.

Kobayashi, H., Masutani, M., Azuhata, S. & Morita, S. 1991 Particle dispersion in a streamwise pressure gradient mixing layer. *Trans. Jpn. Soc. Mech. Engng* **57B,** 1927–1933.

Kocamustafaogullari, G. & Wang, Z. 1991 An experimental study on local interfacial parameters in a horizontal bubbly two-phase flow. *Int. J. Multiphase Flow* **17,** 553–572.

Lance M. & Bataille, J. 1991 Turbulence in the liquid phase of a uniform bubbly air–water flow. *J. Fluid Mech.* **222,** 95–118.

Lee, S. L., Lahey Jr, R. T. & Jones Jr, O. C. 1989 The prediction of two-phase turbulence and phase distribution phenomena using a k–ϵ model. *Jpn. J. Multiphase Flow* **3,** 335–368.

Liu, T. J. & Bankoff, S. G. 1993 Structure of air–water bubbly flow in a vertical pipe—I. Liquid mean velocity and turbulence measurements. *Int. J. Heat Mass Transfer* **36,** 1049–1060.

Marié, J. L. & Lance, M. 1983 Turbulence measurements in two-phase bubbly flows using laser Doppler anemometry. *IUTAM Symp. on Measuring Techniques in Gas–Liquid Two-phase Flows*, p. 141–148.

Mizukami, M., Parthasarathy, R. N. & Faeth, G. M. 1992 Particle-generated turbulence in homogeneous dilute dispersed flow. *Int. J. Multiphase Flow* **18,** 397–412.

Modarress, D., Tan, H. & Elghobashi, S. 1984 Two-component LDA measurement in a two-phase turbulent jet. *AIAA J* **22,** 624–630.

Mori, K. & Sano, M. 1981 Process kinetics in injection metallurgy. *Tetsu-to-Hagané* **67,** 672–695.

Mostafa, A. A. 1992 Turbulent diffusion of heavy-particles in turbulent jets. *Trans. ASME J. Fluids Engng* **114,** 667–671.

Ohba, K. & Yuhara, T. 1982 Study of bubbly flow in vertical tube using LDV. II (Turbulence structure in bubbly flow in square duct). *Trans. Jpn. Soc. Mech. Engng* **48B,** 78–87.

Panchapakesan, N. R. & Lumley, J. L. 1993 Turbulence measurements in axisymmetric jets of air and helium. Part 1. Air jet. *J. Fluid Mech.* **246,** 197–223.

Parthasarathy, R. N. & Faeth, G. M. 1987 Structure of particle-laden turbulent water jets in still water. *Int. J. Multiphase Flow* **13,** 699–716.

Sawada, I., Tani, M., Szekely, J. & Ilegbusi, O. J. 1991 Recent developments and possibilities of computational fluid dynamics in materials processing. *Tetsu-to-Hagané* **77,** 1234–1242.

Serizawa, A., Kataoka, I. & Michiyoshi, I. 1975a Turbulence structure of air–water bubbly flow—I. Measuring techniques. *Int. J. Multiphase Flow* **2,** 221–233.

Serizawa, A., Kataoka, I. & Michiyoshi, I. 1975b Turbulence structure of air–water bubbly flow—II. Local properties. *Int. J. Multiphase Flow* **2,** 235–246.

Serizawa, A., Kataoka, I. & Michiyoshi, I. 1975c Turbulence structure of air–water bubbly flow—III. Transport properties. *Int. J. Multiphase Flow* **2,** 247–259.

Sheng, Y. Y. & Irons, G. A. 1991 A combined laser Doppler anemometry and electrical probe diagnostic for bubbly two-phase flow. *Int. J. Multiphase Flow* **17,** 585–598.

Sheng, Y. Y. & Irons, G. A. 1992 Measurements of the internal structure of gas–liquid plumes. *Metall. Trans.* **23B,** 779–788.

Sun, T-Y. & Faeth, G. M. 1986a Structure of turbulent bubbly jets—I. Methods and centerline properties. *Int J. Multiphase Flow* **12,** 99–114.

Sun, T.-Y. & Faeth, G. M. 1986b Structure of turbulent bubbly jets—II. Phase property profiles. *Int. J. Multiphase Flow* **12,** 115–124.

Szekely, J., Carlson, G. & Helle, L. 1988. *Ladle Metallurgy*. Springer, Berlin.

Theofanous, T. G. & Sullivan, J. 1982 Turbulence in two-phase dispersed flow. *J. Fluid Mech.* **116,** 343–362.

Tsuji, Y. & Morkikawa, Y. 1982 LDV measurements of an air–solid two-phase flow in a horizontal pipe. *J. Fluid Mech.* **120,** 385–409.

Tsuji, Y., Morikawa, Y. & Shiomi, H. 1984 LDV measurements of an air–solid two-phase flow in a vertical pipe. *J. Fluid Mech.* **139,** 417–434.

Wang, S. K., Lee, S. J., Jones Jr, O. C. & Lahey Jr, R. T. 1987 3D turbulence structure and phase distribution measurements in bubbly two-phase flows. *Int. J. Multiphase Flow* **13,** 327–343.

Wygnanski, I. & Fiedler, H. 1969 Some measurements in the self-preserving jet. *J. Fluid Mech.* **38,** 577–612.

Yarin, L. P. & Hetsroni, G. 1994a Turbulence intensity in dilute two-phase flows—1. Effect of particle-size distribution on the turbulence of the carrier fluid. *Int. J. Multiphase Flow* **20,** 1–15.

Yarin, L. P. & Hetsroni, G. 1994b Turbulence intensity in dilute two-phase flows—3. The particles–turbulence interaction in dilute two-phase flow. *Int. J. Multiphase Flow* **20,** 27–44.

Yuan, Z. & Michaelides, E. E. 1992 Turbulence modulation in particulate flows—a theoretical approach. *Int. J. Multiphase Flow* **18,** 779–785.